Supporting Information

Hashimoto et al. 10.1073/pnas.1717363115

SI Materials and Methods

Cell Culture. The human prostatic carcinoma cell lines C4, C4-2, and C4-2B were kind gifts from Leland W. K. Chung, Cedars-Sinai Medical Center, Los Angeles, CA (15). VCaP was a kind gift from Yutaka Kondo, Nagoya University, Nagoya, Japan. MDA-PCa-2b was purchased from the ATCC (CRL-2422). DU-145 was a kind gift from Soichiro Yoshida, Tokyo Medical and Dental University, Tokyo, Japan. PC-3-Luc was purchased from the Japanese Collection of Research Bioresourcest (JCRB1406). The human breast adenocarcinoma cell line MDA-MB-231-Luc was purchased from Cell Biolabs (AKR-231). The human myeloma cell lines KMS11 and U266 were kind gifts from Yoichi Imai, Tokyo Women's Medical University, Tokyo, Japan. The human osteosarcoma cell line SaOS2 was a kind gift from Junya Toguchida, Kyoto University, Kyoto, Japan. The immortalized hMSC UCB408E6E7TERT-33 was purchased from Riken BRC (RCB2080). The human prostate epithelial cell line RWPE-1 was purchased from the ATCC (CRL-11609).

To visualize the exosomes, CD63 fused with improved yellow fluorescent protein (CD63-Venus) or red fluorescent protein (CD63-tdTomato) was stably transduced using a retroviral infection system into MDA-MB-231 cells or C4-2B cells.

To establish cell clones stably overexpressing hsa-miR-940 hMSCs or MDA-MB-231 cells were transduced with the sequence of pri-mir-940 using a lentiviral infection system. A genomic fragment of human pri-mir-940 was amplified by PCR and cloned into pLenti6.3/V5-DEST (Invitrogen). The target genes of hsa-miR-940, *ARHGAP1* or *FAM134A*, were also infected into hMSCs using the same transduction system. The pLenti6.3/V5-DEST (empty vector)-infected cells were established as a control. In contrast, to knock down the targets, hMSCs were transfected with Silencer Select siRNA-ARHGAP1 and siRNA-FAM134A (s1584 and s35603; Thermo Fisher Scientific) using Lipofectamine RNAiMAX (Invitrogen) according to the manufacturer's instructions.

Osteogenic Differentiation. hMSCs were seeded in 24-well plates at 4×10^4 cells per well and then transiently transfected with 20 nM miRNA mimics (Dharmacon) using HiPerFect (Qiagen) or 20 nM siRNAs (Thermo Fisher Scientific) using RNAiMAX (Invitrogen) according to the manufacturer's instructions. Cells were cultured in Minimum Essential Medium Eagle (α-MEM; Wako) containing 50 μM ascorbic acid 2-phosphate, 5 mM β-glycerophosphate, and 100 nM dexamethasone, as previously reported (33). Culture medium was changed every 3 d, and miRNA mimics were added to the medium every week. Osteogenic differentiation potential was examined by ALP assay and von Kossa staining, as previously described (12). The expression of osteogenic markers was investigated using qPCR analysis. The mineralized area of the differentiated cells was quantified using ImageJ (35).

Osteoclast Differentiation. Peripheral blood mononuclear cells (PBMCs) were isolated from human peripheral blood using Lymphoprep (Cosmo Bio Co., Ltd.), according to the manufacturer's instructions. Then, $CD14^+$ cells were separated from PBMCs by magnetic-activated cell sorting, as previously reported (36). Cells were seeded in 48-well plates at 5×10^4 cells per well and transiently transfected with 20 nM miRNA mimics using HiPerFect. Cells were cultured in α-MEM (Gibco) supplemented with 10% FBS (SAFC Bioscience) in the presence of 10 ng/mL human macrophage colony-stimulating factor (M-CSF; R&D Systems) for 2 d and then differentiated into osteoclasts by exposure to 30 ng/mL human RANKL (Peprotech) and 10 ng/mL M-CSF. Differentiated osteoclasts were stained by TRAP staining, and the number of $TRAP^+$ multinucleated cells was counted as previously described (12). The expression of an osteoclast marker; *CTSK* was also investigated using quantitative PCR analysis.

Exosome Isolation. Exosomes were isolated as previously reported (34). Briefly, cells were cultured in Advanced DMEM (Gibco) without FBS for 48 h before the isolation. The cultured medium was centrifuged at $2{,}000 \times g$ for 15 min to remove dead cells, and then, the supernatant was centrifuged at $12{,}000 \times g$ for 30 min to remove cell debris. After centrifugation, the supernatant was filtered using a 0.22-μm polyvinylidene fluoride (PVDF) filter and ultracentrifuged at $100{,}000 \times g$ for 70 min. The pellet was washed with PBS, and the resuspended solution was ultracentrifuged again at $100{,}000 \times g$ for 70 min. Finally, the pellet was resuspended with PBS again. All ultracentrifugation steps were performed at 4 °C using Optima XE-90 (Beckman Coulter). The concentration and particle size distribution of isolated exosomes were identified by Nanoparticle Tracking Analysis (NanoSight).

Exosome Transfer Assay. Exosomes from C4-2B-CD63-Venus cells were isolated and added to tdTomato-expressing hMSCs. hMSCs were seeded in six-well plates at 3×10^4 cells per well and cultured in α-MEM supplemented with exosome-free FBS (Thermo Fisher Scientific). We examined the transfer of Venus-labeled exosomes using a confocal microscope A1R (Nicon) at 24 h after the addition of the exosomes.

miRNA Microarray Analysis. To perform microarray analysis, exosomal or cellular total RNAs were extracted using miRNeasy Mini Kit (Qiagen). The following cancer cell lines were used: the prostate adenocarcinoma cell lines C4, C4-2, and C4-2B (five different clones each); the breast adenocarcinoma cell line MDA-MB-231-Luc (two different clones); the myeloma cell lines KMS11 and U266 (two different clones each); and HEK293 cells as a normalization control. The quality and purity of the extracted RNAs were measured using an Agilent 2100 Bioanalyzer (Agilent Technologies). Microarray analysis was performed using Agilent Human miRNA Microarray Kit (V3), and we used a sample input of 100 ng of each total RNA. Briefly, the samples were first dephosphorylated by calf intestine phosphatase, and 3′ ends of the dephosphorylated samples were labeled with cyanine 3-cytidine biphosphate using T4 RNA ligase. The labeled miRNA was hybridized to microarray glass slides in a hybridization rotator for 20 h at 55 °C with 20 rotations per minute, and then washed with two types of buffers (Gene Expression Wash Buffers 1 and 2; Agilent Technologies). The dried glass slides were scanned with Agilent Microarray Scanner (Agilent Technologies) with default settings, and the data were extracted using Feature Extraction software v11.0.1.1 (Agilent Technologies). The data were subsequently normalized and analyzed using GeneSpring GX software (Agilent Technologies) and converted into heat map using R v3.3.1 (37).

Cancer Cell Implantation. C4-2B or MDA-MB-231 cells ($0.5–1 \times 10^6$ cells/5 μL in PBS) were injected into the tibiae of NOD/SCID or BALB/cAJcl-nu/nu mice, as previously described (38). hsa-miR-940–overexpressing MDA-MB-231 cells (1×10^6 cells/100 μL in Matrigel) were also implanted on the calvaria of BALB/cAJcl-nu/nu mice, as previously reported (21). All animal

experiments were performed with approval from the Animal Study Committee of Tokyo Medical and Dental University and conformed to the relevant guidelines and legislations.

Micro-CT Analysis. Micro-CT analysis was performed using R_mCT2 (Rigaku) with an isometric resolution of 40 μm, or ScanXmate-L090 (Comscan) with an isometric resolution of 12 μm. The micro-CT files were reconstructed as TIFF images and transferred to TRI/FCS-BON (Ratoc System Engineering) for the quantitative analysis. We measured the mineralized tissue volume using a calibration curve obtained from a BMD phantom (Ratoc).

Histology and Immunohistochemistry. To perform histological analyses of induced osteoblastic lesions, H&E and von Kossa staining were performed using paraffin and undecalcified sections, respectively, according to standard protocols (39). Immunohistochemistry was performed on frozen sections as previously described (38). Anti-ALP primary antibody was a kind gift from Kimimitsu Oda, Niigata University Graduate School of Medical and Dental Sciences, Niigata, Japan (40). Sections were examined using a fluorescence microscope (BZ-9000; Keyence) or a confocal microscope (A1R; Nicon), and analyzed using ImageJ (35).

Cell Sorting. Two weeks after the implantation of miR-940–overexpressing MDA-MB-231-CD63-tdTomato cells, the developed tumors were harvested from GFP-transgenic nude mice. The tumors were digested into individual cells with 10 mg/mL of collagenase IV (Worthington), 2.4 U/mL of dispase (Becton Dickinson), and 0.05% trypsin. Cells were suspended in ice-cold HBSS containing 2% FBS and 1% penicillin/streptomycin and then stained for 30 min on ice with a following antibodies: PE-cy7–conjugated anti-CD45; PE-cy7–conjugated anti-Ter119 (for hematopoietic cells); and PE-cy7–conjugated anti-CD31 (for endothelial cells) (Becton Dickinson). Propidium iodide (PI, 2 μg/mL; Sigma) was used to eliminate dead cells. To isolate the GFP-expressing host stromal cells and tdTomato-expressing transplanted cells, we sorted $CD31^-$ $CD45^-$ $Ter119^-$ GFP^+ cells and $CD31^-$ $CD45^-$ $Ter119^-$ $tdTomato^+$ cells using a BD FACSAria II (Becton Dickinson). Analysis of sorted cell populations routinely demonstrated 99% purity. We also isolated $Venus^+$ exosomes derived from MDA-MB-231-CD63-Venus cells transfected with miR-940 or control mimic. The culture media was changed 24 h after transfection, and the transfected cells were subsequently cultured for 48 h. Exosome preenriched solution was obtained by ultracentrifugation of the culture supernatant and incubated with streptavidin-coated beads (Exosome-Dynabeads, Streptavidin for Isolation/Detection; Invitrogen) coated with anti-human CD63-biotin for 18–22 h at 4 °C with mixing. The $Venus^+$ exosomes bound to the beads were isolated using flow cytometry.

Quantitative Real-Time PCR. Total RNA from exosomes or cultured cells was extracted using miRNeasy Mini Kit (Qiagen), TRIZOL (Thermo Fisher Scientific Inc.), or NucleoSpin miRNA (Takara), according to the manufacturer's instructions. The RNA quality and quantity were measured using a Quant-iT RNA Assay Kit (Invitrogen) or a NanoDrop 2000 spectrophotometer (Thermo Fisher Scientific).

To analyze the expression of miR-940, RNAs were reverse-transcribed using miScript II RT Kit (Qiagen), and relative miRNA expression levels were determined by real-time quantitative PCR (qPCR) using miScript SYBR Green PCR Kit (Qiagen). The following primers were used for the qPCR: Hs_RNU6-2_11 and Hs_miR-940_3 (MiScript Primer Assay; Qiagen). To examine the expression of pri-mir-940, RNAs were reverse-transcribed using ReverTra Ace qPCR RT Kit (TOYOBO), and qPCR was performed using the TaqMan Pri-miRNA Assays (Applied Biosystems). The following primers were used: *GAPDH* and hsa-mir-940 (TaqMan Pri-miRNA Assays; Applied Biosystems). To analyze the expression of osteogenic and osteoclastic markers or hsa-miR-940 target genes, RNAs were reverse-transcribed using ReverTra Ace, and the qPCR was performed using the Brilliant III Ultra-Fast SYBR Green QPCR Master Mix (Agilent Technologies). The following primers were used: *GAPDH* S, 5′-ACCCAGAAGACTGTGGATGG-3′ and AS, 5′-CACGTTGGCAGTGGGGACAC-3′; *ALPL* S, 5-TCCAGGGATAAAGCAGGTCTT-3′ and AS, 5′-TGGTGTTGTACGTCTTGGAGAG-3′; *BGLAP* S, 5′-GTGCAGAGTCCAGCAAAGGT-3′ and AS, 5′-CGATAGGCCTCCTGAAAGC-3′; *CTSK* S, 5′-AGGCTTCTCTTGGTGTCCATAC-3′ and AS. 5′-TGCCAGTTTTCTTCTTGAGTTG-3′; *ARHGAP1* S, 5′-GGAGTTTGACCGCAAGTACAAG-3′ and AS, 5′-GCTCTTCTGTGTGGATTTCAGG-3′; and *FAM134A* S, 5′-CTGACGTTTCAGCATCATCC-3′ and AS, 5′-GAACATAGTGTCCCAACACAGC-3′. We used RNU6-2 (for mature miR-940) and *GAPDH* (for pri-mir-940 and other genes) as internal controls. All qPCR reactions were performed using Mx3000P real-time PCR system (Agilent Technologies), and the ΔΔCt method was used for the data analysis.

Western Blot Analysis. Western blot analysis was performed as previously described (12). We used primary antibodies against ARHGAP1 (sc-109201; Santa Cruz), FAM134A (sc-242687; Santa Cruz), and β-actin (A2228; Sigma). We used β-actin as an internal control for all analyses. Immunoblotting was visualized using Chemi-Lumi One Ultra (Nacalai Tesque Inc.) and analyzed using FUSION SYSTEM (Vilber-Lourmat).

Dual-Luciferase Reporter Assay. Oligonucleotides including the binding site of hsa-miR-940 were purchased from Invitrogen. Human *ARHGAP1* and *FAM134A* 3′UTR regions were amplified by PCR. Then, the oligonucleotides or 3′UTR regions were cloned into the pCMV-Luc reporter plasmid (11). SaOS2 cells were seeded in 24-well plates at 1.0×10^5 cells per well and cotransfected with 50 ng of the reporter plasmid, 40 nM of negative miRNA mimic control or hsa-miR-940 mimic, and 10 ng of phRL-tk plasmid as an internal control, using Hiperfect (Qiagen). After a 48-h transfection, Firefly or *Renilla* luciferase activities were determined by dual-luciferase reporter assay (Promega).

Human Bone Metastasis Specimens. The Cancer Institute of the Japanese Foundation for Cancer Research stocks frozen samples of bone metastasis lesions that were previously harvested from prostate cancer patients. Informed consent for their use in medical research was obtained under an Institutional Review Board-approved protocol. The ethics committee of the Cancer Institute approved the use of such samples in this study. The expression of miR-940 in the human samples was examined by qPCR.

Cell Viability Assay. The SCADS inhibitor kits consisting of 187 types of anticancer drugs were kindly provided by Molecular Profiling Committee, Grant-in-Aid for Scientific Research on Innovative Areas "Platform of Advanced Animal Model Support" (Japan). miR-940–overexpressing MDA-MB-231 cells or C4-2 cells were seeded in 96-well plates at a concentration of $2–5 \times 10^4$ cells per well and treated with 10 μM of each anticancer drug for 48 h. Cell Counting Kit-8 (Dojindo) was used to assess the viability of the treated cells. The absorbances at a wavelength of 450 nm were measured. DMSO-treated cells were used as a normalization control.

Statistical Analyses. All of the data are presented as the means ± SEM. We performed parametric statistics by Student's t test, one-way ANOVA with Tukey's HSD test, nonparametric statistics by the Mann–Whitney U test, or the Kruskal–Wallis test using R v3.3.1 (37). The values were considered significant at $P < 0.05$. The results are representative of more than three individual experiments.

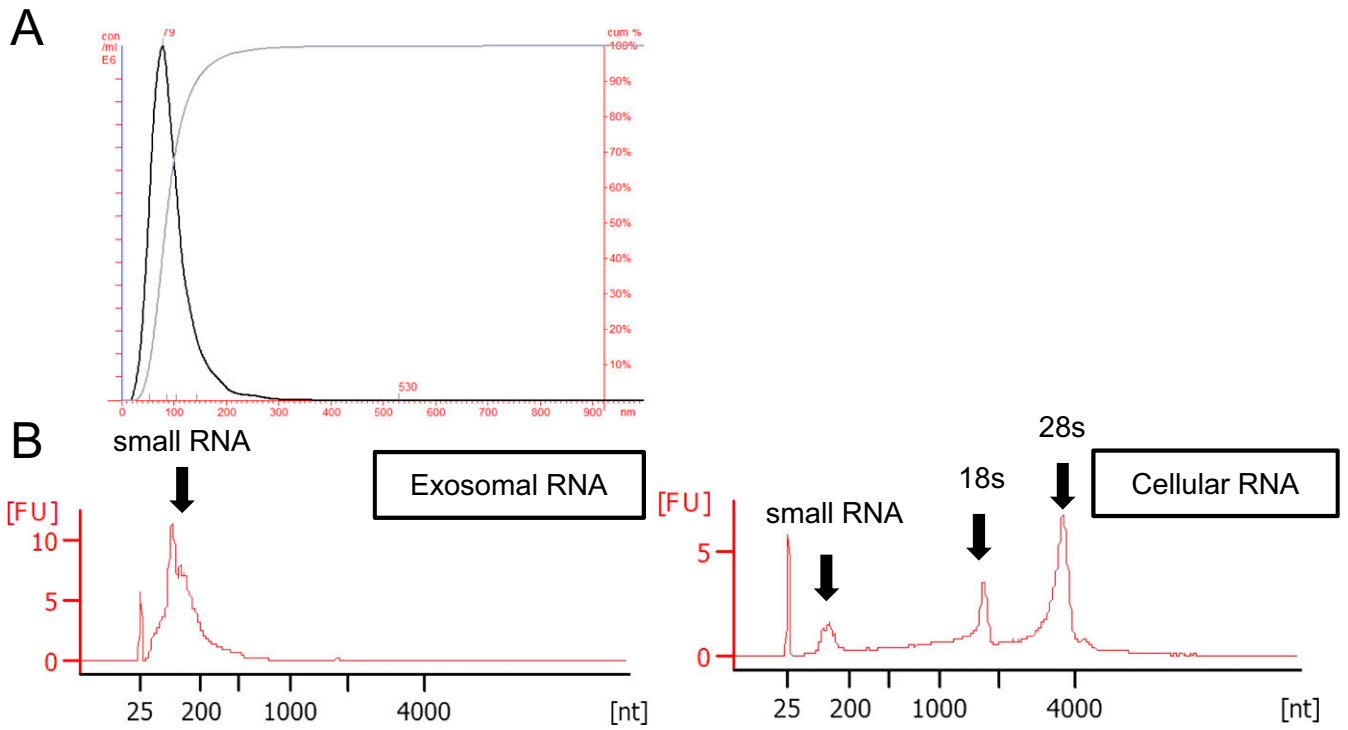

Fig. S1. Characterization of exosomes secreted by cancer cells. (*A*) Size distribution of exosomes isolated from the culture media of C4-2B cells by nanoparticle tracking analysis. (*B*) Representative electropherograms of total RNAs extracted from exosomes secreted by C4-2B cells. The cancer-secreted exosomes were isolated by ultracentrifugation of the culture media. The RNA quality was analyzed using a 2100 Bioanalyzer. Cellular RNAs (*Right*) showed notable 18S and 28S ribosomal RNA bands and a lower level of small RNAs. In contrast, exosomal RNAs (*Left*) were abundant in small RNAs. FU, fluorescence unit; nt, nucleotide. The peak at 25 nt represents the internal standard.

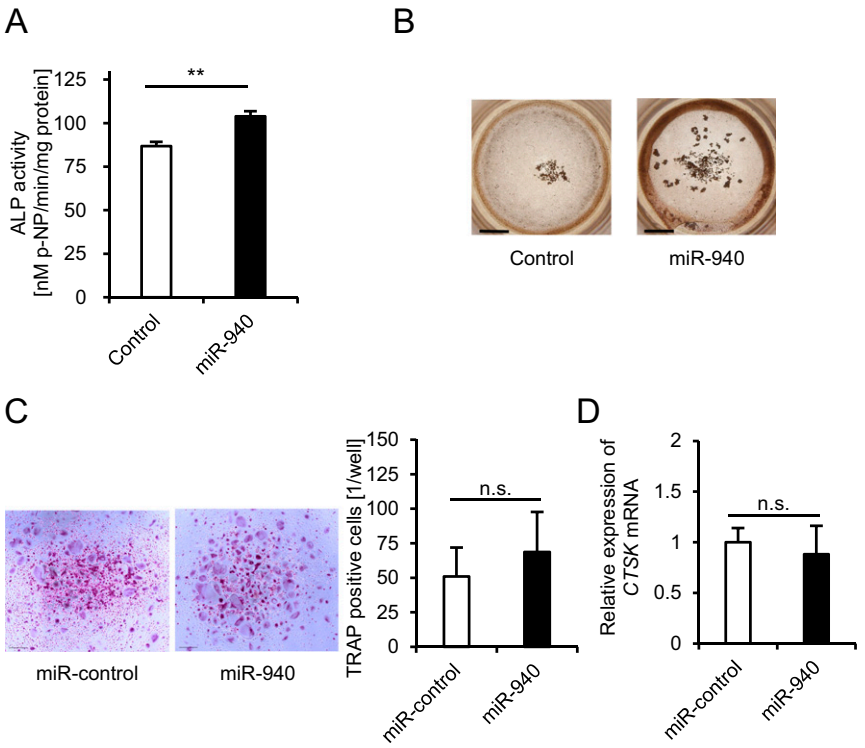

Fig. S2. hsa-miR-940 overexpression promotes hMSC osteogenic differentiation but does not affect osteoclastogenesis. (*A* and *B*) The osteogenic differentiation potential of hMSCs stably overexpressing miR-940 was analyzed by ALP assay and von Kossa staining. (*A*) The ALP assay showed that ALP activity was significantly increased in miR-940–overexpressing cells after 7 d of osteogenic induction. (*B*) von Kossa staining showed that hMSCs overexpressing miR-940 induced more mineralized nodules after 28 d of osteogenic induction compared with the empty vector-infected hMSCs (Control). (Scale bars, 4 mm.) (*C* and *D*) Effects of transient overexpression of miR-940 on osteoclast differentiation. Human osteoclast precursor cells were isolated from $CD14^+$ PBMCs and differentiated into osteoclasts for 7 d. (*C*) The number of $TRAP^+$ multinucleated osteoclasts was not altered by miR-940 overexpression. (Scale bars, 100 μm.) (*D*) qPCR analysis also showed no significant difference in *CTSK* expression. All of the data are the means ± SEMs ($n = 3$). n.s., not significant, $^{**}P < 0.01$ by Student's *t* test (*A*–*D*).

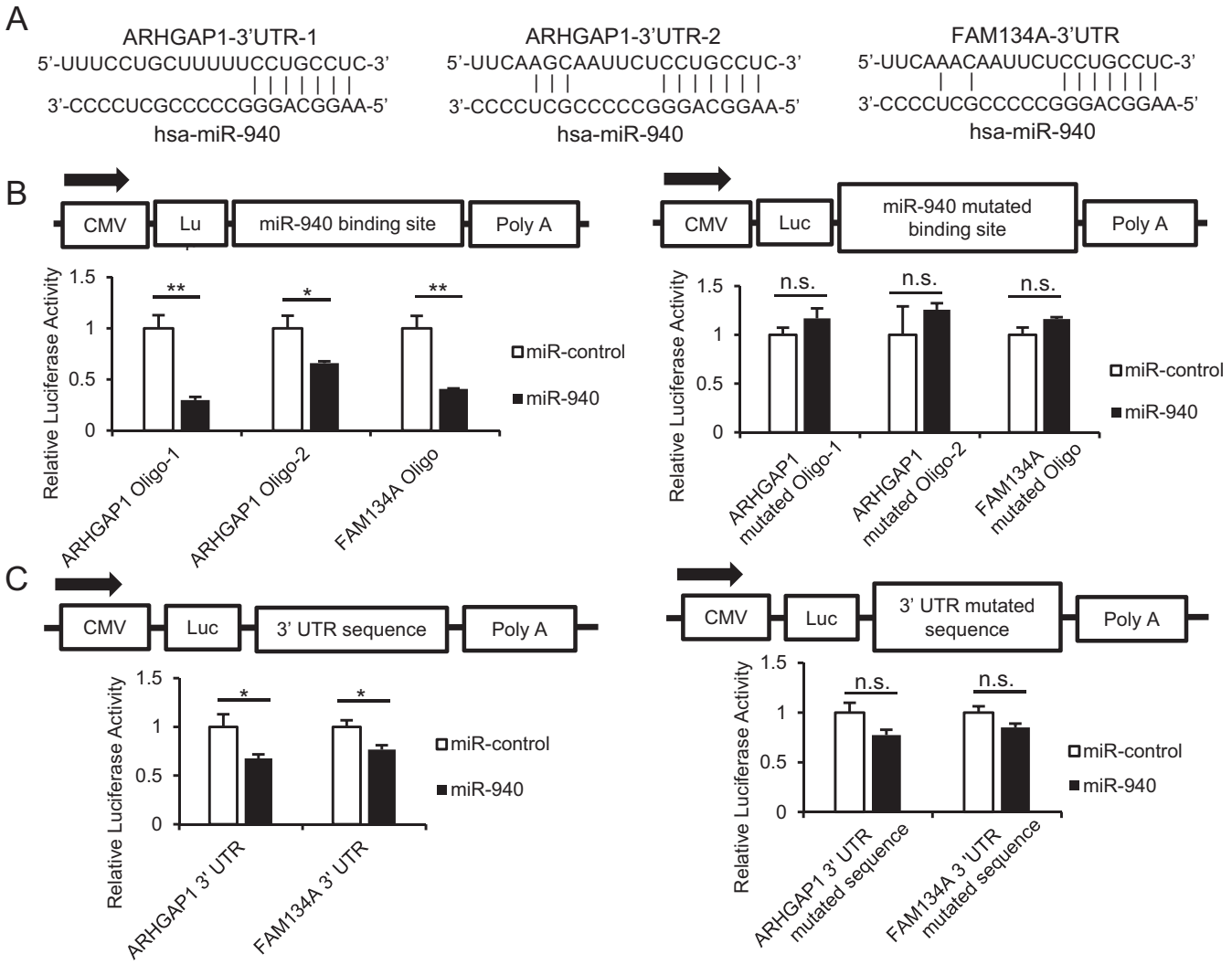

Fig. S3. hsa-miR-940 inhibits *ARHGAP1* and *FAM134A* expression by binding to the 3′UTR sequence. (*A*) A schematic representation of miR-940–binding sites in the 3′ UTR of *ARHGAP1* or *FAM134A* mRNA. (*B* and *C*) SaOS2 cells were cotransfected with the reporter plasmids and miRNA mimics. After cotransfection for 48 h, a luciferase assay was performed. The firefly luciferase signal was normalized to the *Renilla* luciferase signal. CMV; cytomegalovirus promoter, Luc; luciferase. (*B*) Inhibitory effect of the transient overexpression of miR-940 on luciferase reporter activities mediated by the miR-940-binding sites of *ARHGAP1* or *FAM134A* mRNA (*Left*) or the mutated binding sites (*Right*). (*C*) Inhibitory effect of the transient overexpression of miR-940 on luciferase reporter activities mediated by the entire 3′UTR sequence of *ARHGAP1* or *FAM134A* mRNA (*Left*) or the mutated sequence (*Right*). The mutated sequences were generated by a three-base deletion in each seed sequence. All of the data are the means ± SEMs ($n = 3$). n.s., not significant; $^{*}P < 0.05$, $^{**}P < 0.01$ by Student's t test (*B* and *C*).

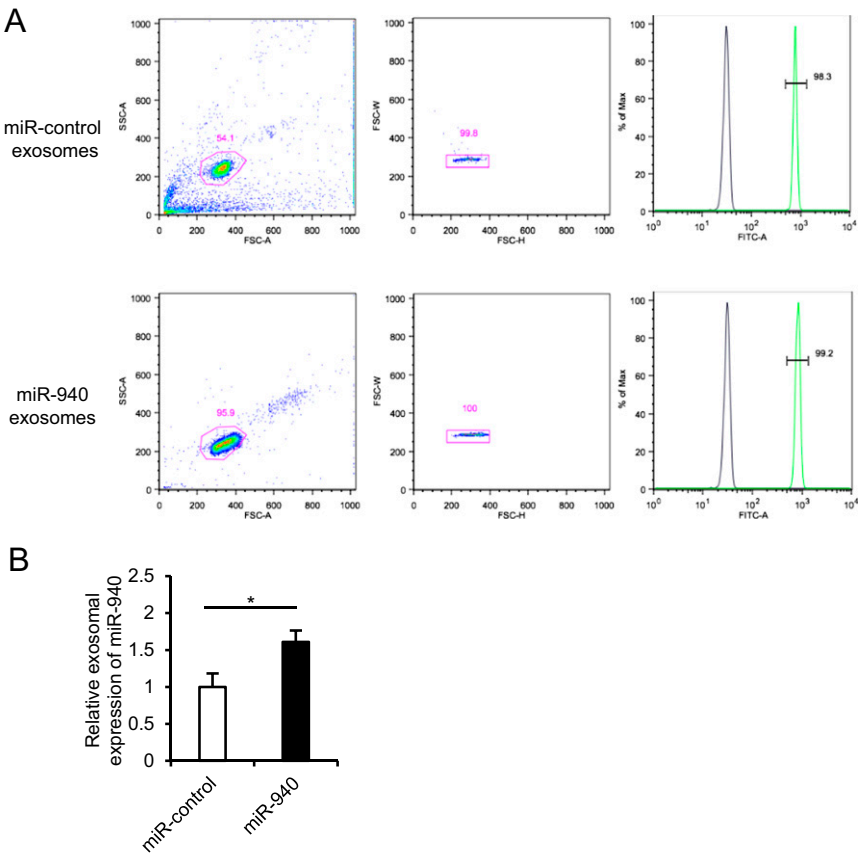

Fig. S4. hsa-miR-940 is enriched in exosomes secreted by miR-940–overexpressing MDA-MB-231 cells. MDA-MB-231-CD63-Venus cells were transfected with miR-940 or control mimic and cultured for 48 h, and Venus$^+$ exosomes were isolated from the culture supernatant by flow cytometry using magnetic beads coated with anti-human CD63. (*A*) Isolation of exosomes bound to anti-human CD63 beads by flow cytometry. FSC/SSC shows the singlet of bead/exosome complex (*Left* and *Center*). Beads with high Venus expression were sorted by FACSAria (*Right*). Negative control (beads only); black line, and exosome samples; green line. (*B*) qPCR analysis showing that miR-940 was significantly expressed in the exosomes from the MDA-MB-231 cells transfected with miR-940 mimic. Data are the mean ± SEM ($n = 3$); $^*P < 0.05$ by Student's *t* test.

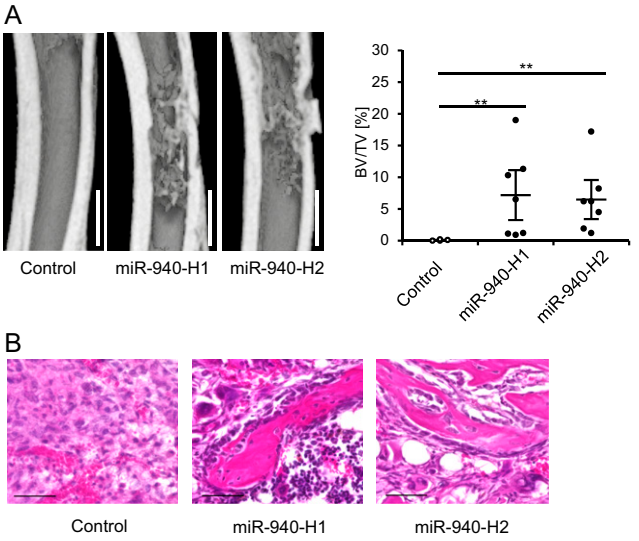

Fig. S5. hsa-miR-940–overexpressing MDA-MB-231 cells also induce osteoblastic lesions in tibial sites. miR-940-overexpressing MDA-MB-231 cells were injected into the tibiae of nude mice. (*A*) Representative micro-CT images of mouse tibiae at 3 wk after intratibial injection of 5×10^5 cancer cells into nude mice. The implanted miR-940–overexpressing cells induced extensive osteoblastic lesions inside the tibiae (*Left*). The volume of mineralized tissues was measured (*Right*). (Scale bars, 1 mm.) (*B*) Representative H&E staining of the osteoblastic lesions. (Scale bars, 50 μm.) All of the data are the means ± SEMs ($n = 4$–7). $^*P < 0.05$, $^{**}P < 0.01$ by the Kruskal–Wallis test with the Mann–Whitney *U* test.

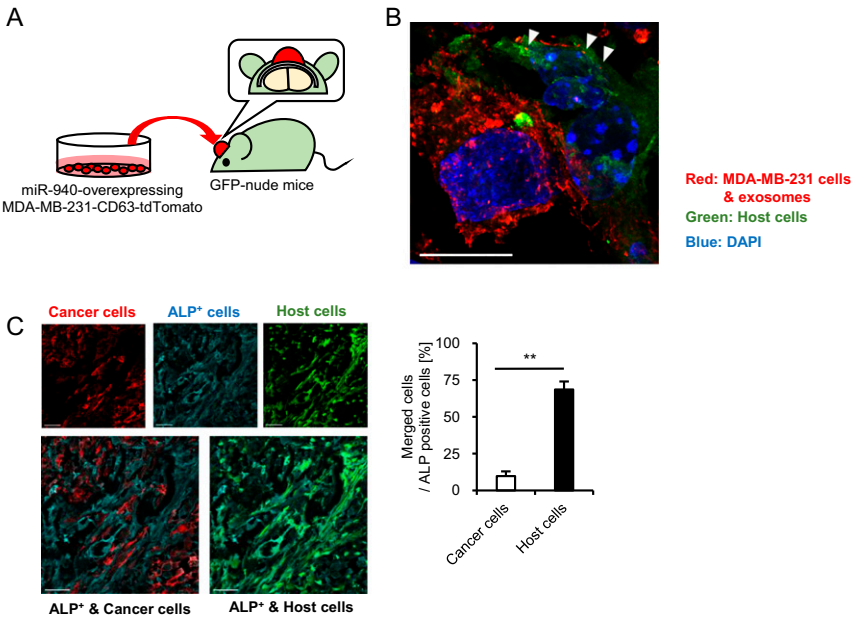

Fig. S6. Cancer cell-derived exosomes induce the osteogenesis of host cells in the bone microenvironment. miR-940–overexpressing MDA-MB-231-CD63-tdTomato cells were implanted on the calvarial bones of 10-wk-old ubiquitously GFP-expressing nude mice. (*A*) A diagram illustrating the design of in vivo experiments. (*B*) Confocal microscopy image showing that tdTomato-labeled exosomes secreted by MDA-MB-231-CD63-TdTomato cells were incorporated into GFP-expressing host cells. White arrowheads indicate tdTomato-labeled exosomes. (Scale bar, 10 μm.) (*C*) Confocal microscopy images of immunofluorescent staining using a primary antibody against ALP. GFP-expressing host cells around the osteoblastic lesions expressed ALP, suggesting that the ALP activity of host cells was up-regulated by cancer cell-derived exosomes. The ratio of ALP-positive cells merged with cancer or host cells was analyzed using ImageJ (*Right*). (Scale bars, 50 μm.) All of the data are the means ± SEMs ($n = 5$). $^{**}P < 0.01$ by the Paired *t* test.

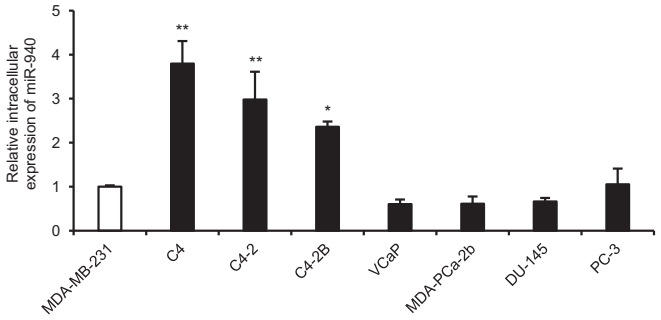

Fig. S7. Relative intracellular expression of hsa-miR-940 in several human prostate cancer cell lines. qPCR analysis showed that C4 cells and its lineage-derived cell lines, C4-2 and C4-2B cells, had higher expression of miR-940 than the other prostate cancer cell lines. All of the data are the means ± SEMs ($n = 3$). n.s., $^{*}P < 0.05$, $^{**}P < 0.01$ by one-way ANOVA with Tukey's HSD test.

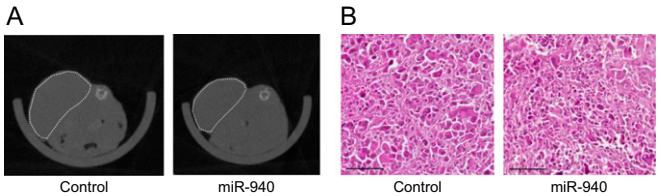

Fig. S8. Osteoblastic lesions induced by hsa-miR-940 might depend on the microenvironment. (*A* and *B*) Implantation of miR-940–overexpressing MDA-MB-231 cells into the subcutaneous tissues of mice. (*A*) Representative axial micro-CT cross-sections of the developed tumors at 8 wk after implantation. The dotted lines indicate the margin of the tumors. (*B*) Representative H&E stains of the developed tumors. miR-940–overexpressing MDA-MB-231 cells did not induce osteoblastic lesions in the subcutaneous tissues. (Scale bars, 100 μm.)

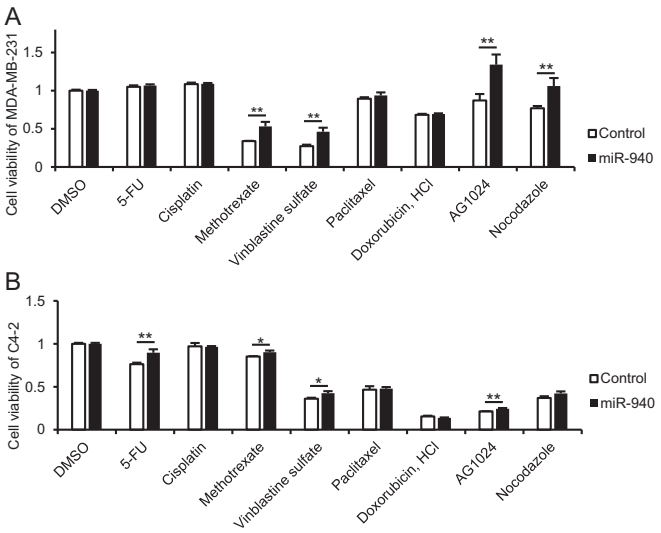

Fig. S9. Cancer cells augmented resistance against chemotherapy agents by hsa-miR-940 overexpression. (*A* and *B*) The effect of hsa-miR-940 on the resistance against anticancer drugs. miR-940–overexpressing MDA-MB-231 cells (*A*) or C4-2 cells (*B*) were seeded into 96-well plates and treated with 187 types of anticancer drugs using a SCADS inhibitor kit. After 48-h culture with each drug, cell viability was measured using a cell-counting kit. miR-940–overexpressing cells showed higher resistance against several chemotherapy agents (e.g., 5-FU, methotrexate, and vinblastine) compared with empty vector-infected cells. AG1024, a selective IGF-1R inhibitor; Nocodazolen, a microtubule-depolymerizing agent. Cells were treated with 10 mM of each drug for 48 h. DMSO-treated cells were used as a control. All of the data are the means ± SEMs ($n = 3$); $*P < 0.05$, $**P < 0.01$ by Student's *t* test.